Physicochemical Studies on Pepsin−CTAB Interaction: Energetics and Structural Changes

ARTICLE *in* THE JOURNAL OF PHYSICAL CHEMISTRY B · APRIL 2007

Impact Factor: 3.3 · DOI: 10.1021/jp066051l · Source: PubMed

4 AUTHORS, INCLUDING:

Indranil Chakraborty
St. Xavier's College, Kolkata
25 PUBLICATIONS **915** CITATIONS
SEE PROFILE

Satya P Moulik
Jadavpur University
297 PUBLICATIONS **7,343** CITATIONS
SEE PROFILE

Article

Physicochemical Studies on Pepsin–CTAB Interaction: Energetics and Structural Changes

Tanushree Chakraborty, Indranil Chakraborty, Satya P. Moulik, and Soumen Ghosh

J. Phys. Chem. B, **2007**, 111 (10), 2736-2746• DOI: 10.1021/jp066051l • Publication Date (Web): 21 February 2007

Physicochemical Studies on Pepsin−CTAB Interaction: Energetics and Structural Changes

Tanushree Chakraborty, Indranil Chakraborty, Satya P. Moulik, and Soumen Ghosh*

Centre for Surface Science, Department of Chemistry, Jadavpur University, Kolkata 700032, India

Received: September 16, 2006; In Final Form: December 13, 2006

The interaction between pepsin and CTAB has been elaborately studied with a number of techniques. The enzyme-induced interaction produced complexes, aggregates, and micelles of CTAB with distinct physicochemical features. It was found that at very low surfactant concentration (much below the critical micellar concentration (cmc) of pure CTAB), the surfactant got adsorbed both in monomeric and lower aggregated forms to the high-energy sites of the native biopolymer, leading to enhanced hydrophobicity of the combine, and hence, lowering of the interfacial (air/solution) tension. This was followed by the formation of a faintly turbid solution of the polymer−surfactant coacervate. The CTAB interacted unfolded pepsin along with the surfactant monomer remained adsorbed at the interface to decrease the interfacial tension (γ) to a low level to produce a break in the γ vs log [CTAB] plot prior to the normally observed extended cmc (cmc_e) in presence of polymers. The cac-like aggregation (as observed in tensiometry and viscometry) was not found in conductometry and microcalorimetry, whereas microcalorimetry evidenced the formation of the cmc_e of CTAB in the presence of the biopolymer. The CTAB influenced structural features of the pepsin were assessed from spectral, viscometric, and circular dichroism measurements.

Introduction

Biopolymer−surfactant interaction is an important field of study. Such interaction can lead to the unfolding of proteins and sometimes their denaturation. The topic has direct relevance to the field of pharmaceutics, paints and coatings, adhesives, oil recovery, etc.[1−8] In general, ionic surfactants interact with proteins and the most studied surfactant is sodium dodecylsulfate (SDS). Other surfactants like bile salts (sodium taurodeoxycholate, in particular), cetyltrimethylammonium chloride (CTAC), cetyltrimethylammonium bromide (CTAB), etc. have also been investigated. Among the proteins, bovine serum albumin (BSA) has been studied the most.[8−14] Other representatives are gelatin (Gn), lysozyme (Lz), hemoglobin, myoglobin, casein, etc. In the 1960s and 1970s Tanford et al.[2,3] carried out extensive investigations on the interaction between surfactants and proteins. Chattoraj et al.[15−18] also elaborately studied the binding and related thermodynamics of biopolymer−surfactant systems. The nature of interaction, effect of ionic strength, interfacial property, conformational change, etc. constitute the various aspects of such studies. In this area, the works of Palacios et al.,[14] Shweitzer et al.,[19] Gelamo et al.,[20] and Honda et al.[21] may be cited as representatives. Green and co-workers[22−24] have elaborately studied the Lz-SDS system. The interaction of Gn and Lz with CTAB was studied microcalorimetrically by Chatterjee et al.[25] The binding between the proteins (β-lactoglobulene, hemoglobin, and Lz) with the surfactants CTAB and SDS was studied by Maulik et al.[18] using ion-selective membrane electrodes. A detailed spectroscopic study on the Lz-SDS system has been reported by Stenstam et al.[26] Thorough study of the interaction of trypsin and papain with SDS has also been recently reported.[27−31]

The globular protein pepsin (EC 3.4.23.1) is a proteolytic enzyme, secreted from the pancreas in the presence of stomach acid. It is a gastric, aspartic protease and one of the three principal protein-degrading enzymes in the digestive system. Pepsin catalyzes the hydrolysis of peptide bonds between two hydrophobic amino acids (Phe-Leu, Phe-Phe, Phe-Tyr). Chemical treatment of pepsin has indicated the participation of the two aspartyl residues (which are widely separated in the linear sequence) in the catalytic action indicating the necessity of globular structure (stabilized mostly by the three disulfide bonds) for its enzyme catalytic activity. Pepsin attacks most of the proteins excepting keratin, nail and other carbohydrate-rich proteins.[32] Pepsin is used in the laboratory analysis of various proteins to cleave bonds involving the aromatic amino acids, phenylalanine, tryptophan, and tyrosine. It is also used in the preparation of cheese and other protein-containing foods. X-ray diffraction study by Tang et al.[33] has confirmed 327 amino acid residues (with 5 tryptophan residues) per polypeptide chain in pepsin, with a molecular weight of 34 644. A minor component of commercially available crystallized pepsin contains two extra alanine-leucine residues at the amino terminus of the moiety.[33] Pepsin is a single-chain phosphoprotein[32] with isoelectric pH (IEP) ∼1. Structurally, its active sites are located in a deep cleft within the molecule.

In our program of studying the biopolymer−surfactant interaction, we are interested in exploring the system with pepsin, which has so far been very limited in study. Herein we report the interaction of the protein with CTAB at different pH values using tensiometry, viscometry, conductometry, UV−vis and fluorescence spectrophotometry, microcalorimetry, and circular dichroism. To the best of our knowledge, such a detailed study has been seldom reported in the literature. We have attempted to understand the interaction behavior of pepsin and CTAB at the air/solution interface and in the bulk in relation to specific and nonspecific interaction; the protein structure has been found to be different in some respects from expectation.

* Address for communication to this author. E-mail: gsoumen70@hotmail.com.

10.1021/jp066051l CCC: $37.00
Published on Web 02/21/2007

Experimental Section

Materials. The cationic amphiphile cetyltrimethylammonium bromide (CTAB) and the biopolymer pepsin used were products of Sigma (USA). They were used as received. All solutions were prepared in doubly distilled water and the pH of the solutions was adjusted by adding hydrochloric acid (SRL, India) and sodium hydroxide (BDH, UK) solution as required, using a Global (India) pH-meter consisting of a glass and Ag/AgCl combined electrode. All the measurements were taken under thermostated conditions with accuracy of ±0.1 K.

Methods

Tensiometry. Tensiometric measurements were taken in a calibrated du Noüy Tensiometer (Krüss, Germany) by ring detachment technique. A 0.01 dL sample of pepsin solution at the desired pH and concentration was taken in the themostated (303 ± 0.1 K) container and 20 mmol dL^{-1} of CTAB solution was stepwise added as required. Measurements were taken allowing 30 min intervals for equilibration. The detailed procedure of the measurement of surface tension has been reported earlier.[34−37] Duplicate experiments were carried out for each run and close resemblance of the data points predicted the usage of any of the single runs. The γ values were accurate within ±0.1 mN m^{-1}.

Viscometry. The viscometric experiments were performed with a Cannon-Fenske capillary viscometer with a flow time of 118 s for 0.01 dL water under thermostated condition at 303 ± 0.1 K. Pepsin solution (0.01 dL) of the desired pH and strength was taken in the viscometer and concentrated surfactant solution was progressively added in stages with a Hamilton microsyringe, and the flow times were measured after thorough mixing and thermal equilibration. Because of very low concentration of the biopolymer, the flow time varied within ±0.5 s and the average of three consecutive measurements was considered for each run. The results were associated with standard deviations of ±5%.

Conductometry. The specific conductance (κ) measurements were taken in a Jenway (UK) conductometer, using a conductivity cell of cell constant 100.0 m^{-1}. The same procedure as in tensiometry of addition of 20 mmol dL^{-1} of CTAB in 0.01 dL of pepsin solution of the desired strength at 303 ± 0.1 K was followed. The accuracy of the measurements was within ±1%. κ values were found stable over time. The measurement details can be found in earlier reports.[34−37]

Absorption Spectrophotometry. A UV−visible (1601) Shimadzu (Japan) spectrophotometer operating in dual beam mode was employed for spectral measurements using a matched pair of quartz cuvettes of path length 0.1 dm under thermostated condition (303 ± 0.1 K). The buffer solution without pepsin acted as the control. Surfactant solution was then progressively added in the sample cell (consisting of 3×10^{-3} dL pepsin solution) as required. Optical density at each stage of surfactant addition was measured in the wavelength range of 200−400 nm after thorough mixing. λ_{max} was found to be centered at 280 nm (tryptophan and tyrosine absorption) and varied only slightly during surfactant addition at different pH while the absorbance progressively changed.

Fluorimetry. The fluorimetric experiments were performed on an instrument from Kontron SFM25, Italy, using a quartz cuvette of path length 0.1 dm. The experimental procedure was similar to that of the absorption experiment discussed earlier. The solution was excited at 280 nm and the fluorescence due to the tryptophan and tyrosine residues was measured in the range of 285−450 nm. The λ_{max} for the emission was found at 360 nm. The fluorescence intensity at λ_{max} vs [CTAB] profile was constructed similar to the absorption experiment.

Microcalorimetry. An OMEGA, ITC, microcalorimeter of Microcal, Northampton (USA) was used for thermometric measurements. A concentrated solution of the surfactant CTAB (~16 mmol dL^{-1}) was taken in the microsyringe and was added after equal time intervals of 210 s in multiple steps (50 additions) to 1.325×10^{-3} dL of pepsin solution of the desired pH and strength, taken in the calorimeter cell under constant stirring (300 rpm) condition. An identical pepsin solution (1.6×10^{-3} dL) was taken in the reference cell. The heat released at each step of interaction of the surfactant with the pepsin solution was recorded and the enthalpy per mole of CTAB was calculated with the ITC software. The experiment for surfactant dilution was also performed with the same injection matrix as that of the interaction experiment, taking water of respective pH in the reference cell. Each run was duplicated to check reproducibility. The temperature of the Neslab RTE100 circulating water bath was maintained at 303 ± 0.1 K; the temperature in the cell compartment in the calorimeter was automatically adjusted to an accuracy of ±0.01 K. The enthalpy of interaction was obtained by subtracting the heat of surfactant dilution in water from the heat associated with surfactant dilution in pepsin solution.

Circular Dichroism. Far- and near-UV circular dichroism (CD) experiments were performed in a Jasco, J-600 recording spectropolarimeter (Japan) attached with a chiller to control the temperature of the Xe-lamp and electronic circuit. The instrument was calibrated with an aqueous solution of d_{10}-camphor-sulfonic acid, using a slit width of 1 nm and a scan speed of 50 nm min^{-1}. A sample of 1×10^{-3} dL of 5×10^{-5} kg dL^{-1} of pepsin at a particular pH was taken in a cuvette of 0.01 dm path length for measuring the far-UV CD spectra in the range between 200 and 250 nm and consequently 2 and 130 μL of 10 mmol dL^{-1} CTAB was added to study the conformational changes in the secondary structures of pepsin in the presence of lower and higher concentration of the surfactant. For near-UV CD spectra, 2.5×10^{-3} dL of pepsin of the desired pH was taken in a cuvette of 0.1 dm path length and scanned in the range of 250−320 nm. Both 5 and 250 μL of 10 mmol dL^{-1} CTAB were added to study the conformational changes in the tertiary structure of pepsin at the cac and c_S conditions, respectively. Measurements were taken at pH 3, 4, 6, and 8. The reported spectra were the average of 5 scans.

Results and Discussion

1. Interfacial Properties. *A. Tensiometry.* a. Pure CTAB. Surfactants, in aqueous solution, preferentially adsorb at the air/solution interface owing to their amphiphilic character. This decreases the cohesive interaction among water molecules at the air/solution interface and hence lowers surface tension of water on progressive addition of surfactants up to complete saturation of the interface. Beyond this limit, surfactants self-aggregate and populate the bulk solution without affecting the interface. The threshold concentration required for the self-aggregation is called the critical micellar concentration (cmc) and can be obtained from the break in the γ vs log [surfactant] profile.[34−37] The tensiometric profiles for pure CTAB at pH 3 and 4 are exemplified in Figure 1A. The cmc was found to increase with pH (Table 1).

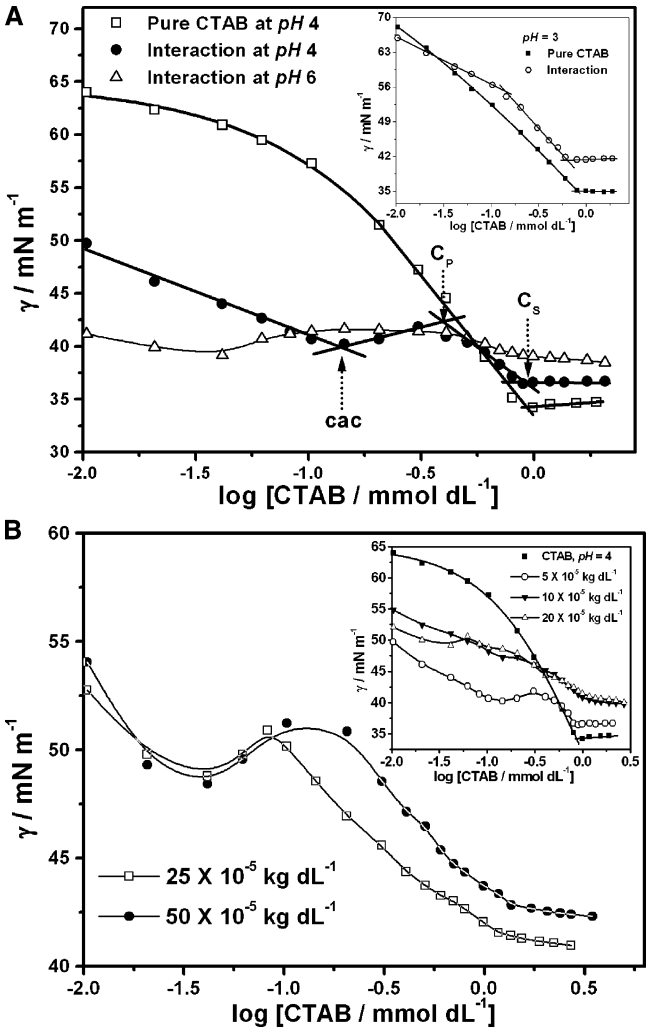

Figure 1. Tensiometric profile for pepsin−CTAB interaction at 303 K: (A) For 5×10^{-5} kg dL^{-1} pepsin at pH 4 and 6; cac, c_P, and c_S are shown in the profile at pH 4. The dilution experiment of pure CTAB in water of pH 4 has also been documented. The inset shows the dilution profile of CTAB in pepsin and water at pH 3. (B) For 25×10^{-5} and 50×10^{-5} kg dL^{-1} pepsin at pH 4. The inset shows a similar plot at 5×10^{-5}, 10×10^{-5}, and 20×10^{-5} kg dL^{-1} pepsin along with that of pure CTAB at pH 4.

The Gibbs surface excess at cmc (Γ_{max}) was calculated from the linear part of the γ vs log [CTAB] plots, using the relation

$$\Gamma_{max} = -\frac{1}{2.303nRT} \lim_{[CTAB]\sim cmc} \frac{d\gamma}{d \log[CTAB]} \qquad (1)$$

where n, R, and T are the number of ionic species per CTAB monomer in solution, the universal gas constant, and absolute temperature, respectively. In this equation, concentration has been used in place of activity since the solutions in use were fairly dilute. The area of exclusion per monomer at the saturated air/solution interface was calculated by using eq 2.

$$A_{min} = \frac{10^{18}}{N\Gamma_{max}} \text{ nm}^2 \text{ molecule}^{-1} \qquad (2)$$

The Γ_{max} and A_{min} values are also reported in Table 1. The A_{min} values increased on increasing pH, consequently a lower number of surfactant-monomers were accommodated at the air/solution interface at elevated pH. The preferential adsorption at the air/solution interface will be quantified in a later section in terms of free energy of interfacial adsorption (ΔG^0_{ad}).

TABLE 1: Critical Micellar Concentration (cmc) and Other Physicochemical Parameters of CTAB at Different pH Values with Different Techniques at 303 K[a]

method		pH 3	pH 4	pH 6	pH 8
tensiometry	cmc	0.80	0.92	1.06	1.13
	γ_{cmc}	35.1	34.2	33.4	34.3
	$\Gamma_{max} \times 10^6$	2.24	2.34	2.03	1.79
	A_{min}	0.71	0.74	0.82	0.93
viscometry	cmc	0.76	0.87	0.99	1.01
conductometry	cmc	0.82	0.98	1.01	1.03
	f	0.96	0.75	0.72	0.69
microcalorimetry	cmc		0.985	1.15	1.18
	ΔH_{cmc}		−9.26	−8.68	−8.40

[a] cmc is given in mmol dL^{-1}; γ_{cmc}, Γ_{max} , and A_{min} values are in mN m^{-1}, mol m^{-2}, and nm^2 molecule^{-1} units, respectively. ΔH_{cmc} is given in kJ mol^{-1}. Standard deviations (SD) for cmc are ±3%, ±5%, ±3%, and ±2% in tensiometric, viscometric, conductometric, and microcalorimetric methods, respectively. SD in γ values is ±2%, and that in ΔH is ±3%.

b. Pepsin−CTAB Interaction. The 5×10^{-5} kg dL^{-1} of pepsin sample has no pronounced surface activity under the studied pHs as evident from the close proximity of γ_{pep} and γ_{H_2O} in Table 2. The lower surface activity suggested the persistence of its native globular form under the studied conditions (Scheme 1A). The peripheral ionic sites of globular pepsin were solvated in solution and the equilibrium constant for the distribution of pepsin in bulk solution was higher than the interfacial population (K_d = [pepsin]^{bulk}/[pepsin]^{interface}) . The increasing surface activity (decreasing γ_{pep}) with increasing [pepsin] resulted in an increase in total analytical [pepsin] in the solution.

At pH 3, pepsin was very close to its IEP and the peripheral negative charge density of the globular biopolymer was small, and consequently the extent of CTA^+ adsorption onto the ionic pepsin sites, dominated by Coulombic interaction, was small. A sharp break in the tensiometric profile of the interaction process was, however, obtained at low [CTAB] regime, which corresponded to the critical aggregation concentration (cac) at ∼0.10 mmol dL^{-1} (inset, Figure 1A). At [CTAB] = 0.68 mmol dL^{-1}, the interaction profile saturated in γ. The air/solution interface was predominantly populated by pepsin−CTAB complex as confirmed by the difference in γ values at the saturation point (for interaction $\gamma \approx 42$ mN m^{-1} and for pure CTAB, $\gamma \approx 35$ mN m^{-1}).

At pH 4, γ_{pep} (∼61.5 mN m^{-1}) droped to ∼50 mN m^{-1} even at 0.01 mmol dL^{-1} [CTAB]. We assume this sudden increase in surface activity was due to adsorption of CTA^+ on the peripheral negatively charged sites and consequent desorption of water of solvation. The peripherally CTA^+ adsorbed globular pepsin thus became hydrophobic and as a whole populated at the air/solution interface, lowering the γ value of the solution (Scheme 1, B). With progressive CTAB addition, this process continued gradually resulting in a decrease in γ up to a certain [CTAB], at which all the peripheral sites were assumed to be saturated with CTA^+. Thereafter, there was an increase in the γ value of the solution. The [CTAB], corresponding to this minimum, corresponded to the critical aggregation concentration, cac. Beyond cac, addition of CTAB led to coacervation and turbidity (out of phase) of the solution, which depleted the pepsin−CTAB complex from the air/solution interface (Scheme 1, C) and resulted in an increase in γ of the solution.

Further CTAB addition led to an increase in surfactant pressure to such an extent that the globular, peripherally CTA^+ adsorbed pepsin started unfolding. This denaturation process was driven by low dielectric constant in the interior of globular

TABLE 2: Determination of Surface Tension Values of Pepsin (γ_{pep}) at Different pH Values and Those of Different Concentrations of Pepsin at pH 4 by Tensiometric Method at 303 K[a]

		5×10^{-5} kg dL^{-1} of pepsin			
pH	3	4	6	8	
γ_{pep}/mN m^{-1}	60.9	61.5	61.9	62.5	
		pH 4			
[pepsin]/kg dL^{-1}	5×10^{-5}	10×10^{-5}	20×10^{-5}	25×10^{-5}	50×10^{-5}
γ_{pep}/mN m^{-1}	61.5	61.4	61.5	60.4	58.4

[a] SD in γ values is ±2%.

SCHEME 1: Pepsin−CTAB Interaction Model in Bulk and at the Air/Water (a/w) Interface[a]

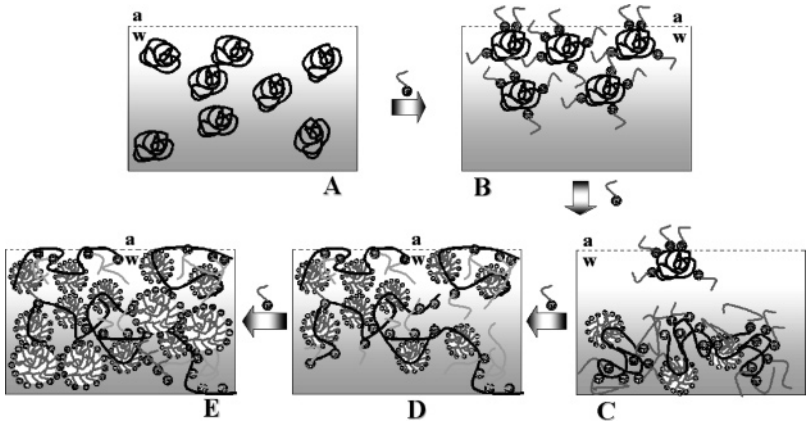

[a] Key: (A) Native globular pepsin in water. **(B)** Peripherally CTAB monomer adsorbed pepsin at the a/w interface and bulk. **(C)** Coacervation leading to depletion of the complex from the interface involving interaction of pepsin with CTAB in both monomeric and aggregated form. **(D)** Unfolding of pepsin to accommodate more monomers and lower aggregates. Hydrophobic segments of pepsin preferentially orient themselves in the air/solution interface to effectively decrease γ. (E) CTAB saturated pepsin followed by formation of free, i.e., larger micelles in solution.

pepsin (∼2,[38] compared to ∼80 for water), which resisted interaction of CTA^+ with the binding sites of the polymer. The unfolding process exposed the interior ionic sites to the solution, which initially increased the degree of solvation, and subsequently resolubilized the pepsin−CTAB complex followed by a second stage of pepsin−CTAB interaction involving the adsorption of lower CTAB aggregates on to the unfolded biopolymer aided both by hydrophobic and ionic interaction (Scheme 1, D). This interaction increased the hydrophobicity of the pepsin−CTAB complex again and the complex finally populated at the air/solution interface. The participation of these complexes to saturate the air/solution interface was evident from the difference in γ values at the point of saturation between the interaction (γ_{cs}) and the micellization (γ_{cmc}) profiles (Table 1 and 3) under similar experimental conditions.

The maximum in tensiometric isotherms corresponded to maximum turbidity of the solution (c_P), and the [CTAB] corresponding to saturation in γ has been termed as the polymer saturation concentration (c_S). Similar interaction behavior was also reported tensiometrically for Lz-SDS,[22,23] poly(*N*-isopropylacrylamide) (PNIPAM)-SDS,[39] acrylamide and acrylamidomethylpropane sulfonate (AM/AMPS)-DTAB,[40] as well as {poly(maleic acid/octylvinylether)} (PVAOME)−$C_{12}E_5$[41] systems. The extended cmc (cmc_e), expected for polymer−surfactant interaction, was absent in the tensiometric profile as reported by Green et al. in Lz-SDS[22,23] interaction and our earlier report of sodium carboxymethylcellulose (NaCMC)−CTAB interaction.[42] The absence of cmc_e signified the absence of collapse of the surfactant-saturated polymer as expected in the classical necklace-bead model.[43] A similar type of bimodal protein−surfactant interaction was also reported by Tanford[2,3] and Turro.[8] BSA−DTAB and BSA−SDS interaction studied by McClement[9] is also worth mentioning. They used microcalorimetry to detect each mode of interaction and differential scanning calorimetry (DSC) to gather information regarding the state of aggregation of the BSA−surfactant complex. In the case of BSA−DTAB interaction, they have also proposed the monomeric adsorption of CTA^+ on to the oppositely charged peripheral sites of native, globular BSA, and a simultaneous unfolding process of the biopolymer.

Variation in pH with 5×10^{-5} kg dL^{-1} of pepsin resulted in a similar pattern in tensiometric isotherms. On increasing alkalinity (pH) of the solution, there was an increase in the negative charge density on pepsin, resulting in a much more

TABLE 3: Critical Concentration of CTAB Required To Induce a Particular Mode of Change in Pepsin (cac, c_S, and c_P) and Other Physicochemical Parameters at Varied pH in the Presence of 5×10^{-5} kg dL^{-1} of Pepsin at 303 K[a]

method		pH 3	pH 4	pH 6	pH 8
tensiometry	cac	0.10	0.15	0.04	0.03
	c_P		0.38	0.34	0.31
	c_S	0.68	0.98	1.01	1.07
	γ_{Cs}	41.0	39.1	39.0	38.7
	$\Gamma^{C_s}_{max} \times 10^6$	1.85	1.41	0.92	0.65
	$A^{C_s}_{min}$	0.90	1.18	1.80	2.56
viscometry	cac	0.16	0.15	0.12	0.10
	c_P	0.45	0.63	0.56	0.49
	c_S	0.94	1.08	1.12	1.16
conductometry	c_P	0.14	0.30	0.34	0.39
	f_{cp}	0.25	0.21	0.18	0.14
	c_S	0.66	1.01	1.04	1.07
	f_{cs}	0.74	0.71	0.71	0.70
UV−VIS spectroscopy	c_P	0.10	0.20	0.30	0.37
	c_S	0.59	-	1.00	1.04
fluorescence spectroscopy	c_P	0.09	0.23	0.13	0.12
	c_S	0.57	-	0.88	0.90

[a] cac, c_P, and c_S are given in mmol dL^{-1}; γ_{cs}, Γ^{cs}_{max}, and A^{cs}_{min} values are in mN m^{-1}, mol m^{-2}, and nm^2 molecule^{-1} units, respectively. SD's for critical concentrations are ±3%, ±5%, and ±3% in tensiometric, viscometric, and conductometric methods, respectively. SD in γ values is ±2%.

TABLE 4: Critical Concentration of CTAB Required to Induce a Particular Mode of Change in Pepsin (cac, c_S, and c_P) and Other Physicochemical Parameters at pH 4 in the Presence of Varied [pepsin] at 303 K[a]

		[pepsin]/kg dL^{-1}				
method		5×10^{-5}	10×10^{-5}	20×10^{-5}	25×10^{-5}	50×10^{-5}
tensiometry	cac	0.15	0.15	0.04	0.03	0.02
	c_P	0.38	0.30	0.07	0.08	0.13
	c_S	0.98	1.07	1.09	1.12	1.23
	γ_{Cs}	39.1	40.3	41.0	42.8	41.4
	$\Gamma^{Cs}_{max} \times 10^6$	1.41	1.07	1.10	0.66	1.12
	A^{Cs}_{min}	1.18	1.55	1.52	2.51	1.48
conductometry	c_P	0.30	0.31	0.37	0.43	0.64
	f_{cp}	0.21	0.33	0.36	0.38	0.39
	c_S	1.01	1.04	1.11	1.16	1.22
	f_{cs}	0.71	0.68	0.62	0.57	0.51

[a] cac, c_P, and c_S are given in mmol dL^{-1}; γ_{cs}, Γ^{Cs}_{max}, and A^{Cs}_{min} values are in mN m^{-1}, mol m^{-2}, and nm^2 molecule^{-1} units, respectively. SD's for critical concentrations are ±3% and ±3% in tensiometric and conductometric methods, respectively. SD in γ values is ±2%.

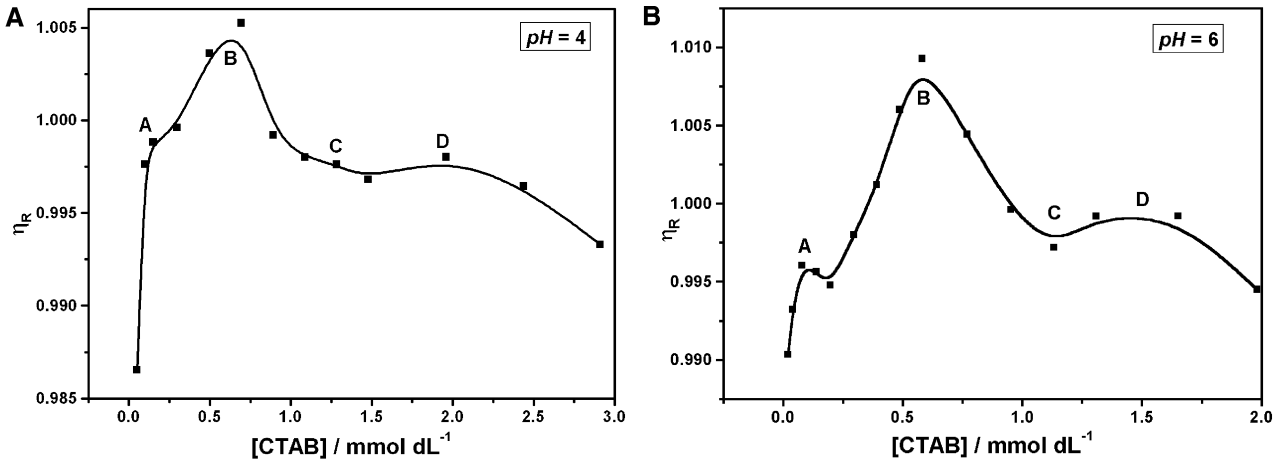

Figure 2. Viscosity of dilution of CTAB in pepsin relative to CTAB dilution in buffer solution (η_R) vs [CTAB] plots at 303 K corresponding to pH 4 (A) and 6 (B).

efficient monomeric adsorption of CTA^+ to the peripheral anionic sites, resulting in increased hydrophobicity and hence a more efficient drop in γ. Very low cac at higher pH values also pointed to stronger, kinetically controlled interaction. The c_P values also decreased with increasing pH; however, c_S increases slightly with increasing pH (Table 3), as expected from an increase in the number of binding sites at enhanced pH values. The decrease in γ_{cs} also indicated more efficient interfacial population by the surfactant-saturated biopolymer.

On increasing [pepsin] at pH 4, the cac and c_P values decreased very sharply, which was expected from a right shift of the pepsin + CTAB ⇔ pepsin−CTAB equilibrium. The c_S value increased with increasing [pepsin] as expected from the mass balance consideration (Table 4).

2. Bulk Properties. *A. Viscometry.* a. Pure CTAB. Addition of CTAB in water (of all the pH values under study) lowered the viscosity of surfactant solution relative to solvent. The minimum in the η_{rel} vs [CTAB] closely resembled the cmc of CTAB (Table 1) in the absence of the biopolymer (plot not shown). The decrease in η_{rel} with increasing [CTAB] in premicellar solution was assumed to be due to lowering in water structure by the hydrophobic tails of surfactant monomers. At the micellar point, the hydrophobic surfactant tail was buried within a hydrophilic shell provided by the surfactant head group and making a change in the course of η_{rel}.

b. Pepsin−CTAB Interaction. The η_R (viscosity of pepsin−CTAB solution relative to the viscosity of CTAB solution) vs [CTAB] plots for the combined systems at the studied pH values of 3, 4, 6, and 8 were found to have characteristic features. The general pattern was the same: a shoulder (A), followed by a crest (B), a trough (C), and another crest (D). Illustrations at pH 4 and 6 are depicted in Figure 2. The [CTAB] at A, B, and C, given in the Table 3, were higher than the cac and c_P values obtained from tensiometry but the c_S values agreed with tensiometry. A comparable change in tensiometry corresponding to the point D (the second crest) in viscometry was not observed in tensiometry. The increased viscosity ratio beyond cac (A) indicated aggregation of the protein by the binding interaction with CTAB, which maximized at B due to aggregation of the pepsin−CTAB complex. Beyond (B), η_R declined by unfolding of the assemblies and the minimum corresponded to c_S. The second crest (D) might be the result of secondary aggregation of the species. The matching of the critical concentrations with the inflections in the viscosity results was interesting and supportive.

B. Conductometry. a. Pure CTAB. The conductometric profiles of pure CTAB at the studied pH values are shown in inset A, Figure 3A. The cmc values corresponding to the breakpoints in the specific conductance (κ) vs [CTAB] plots are reported in Table 1 as expected from the counterion condensation phenomena at micellar interface. The results agreed with the tensiometry. The extent of counterion dissociation (α) was obtained from the slope-ratio method, $\alpha = S_2/S_1$, with S_2 and S_1 being the slopes of the κ vs [CTAB] profile at post- and premicellization stages, respectively. The counterion condensation (f) at the palisade layer around the aggregated micellar structure was obtained from the following relationship,

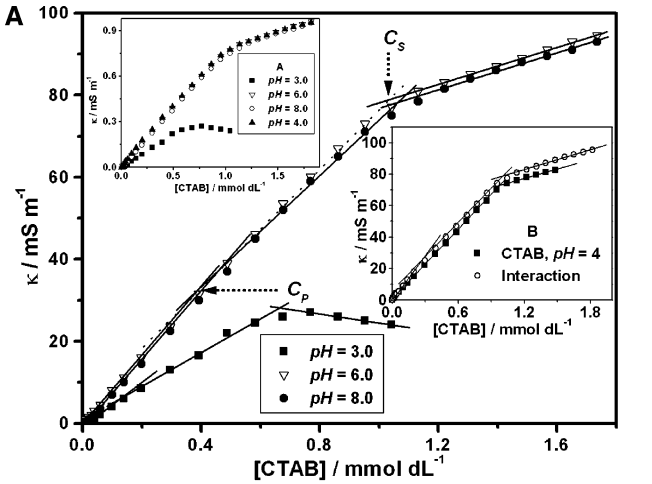

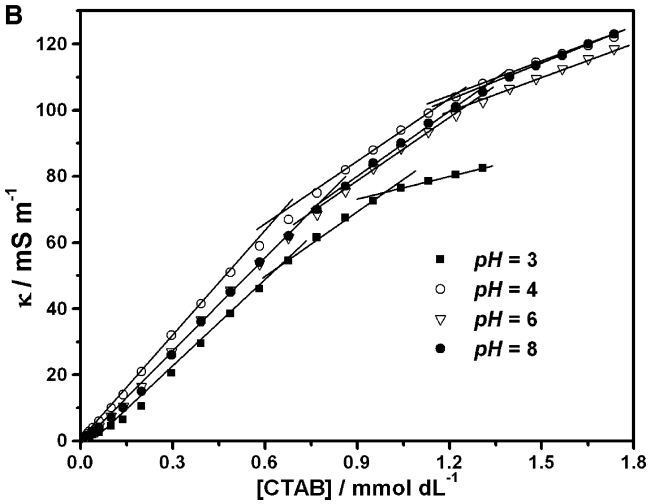

Figure 3. (A) Conductometric profile (at 303 K) of CTAB dilution in 5×10^{-5} kg dL^{-1} of pepsin at varied pH values. Inset A shows the specific conductance (κ) vs [CTAB] profile for pure CTAB dilution at different pH values. Inset B shows the CTAB dilution profile in 5×10^{-5} kg dL^{-1} of pepsin solution and in water at pH 4. (B) Conductometric profile of 50×10^{-5} kg dL^{-1} of pepsin−CTAB interaction course at varied pH (at 303 K).

$f = 1 - \alpha$. The extent of counterion condensation decreased with increasing pH of the solution.

b. Pepsin−CTAB Interaction. The pepsin−CTAB interaction was studied conductometrically at 5×10^{-5} and 50×10^{-5} kg dL^{-1} of pepsin under varied pH values. The results are exemplified in Figure 3, parts A and B, respectively. Inset B in Figure 3A represents a comparative conductance profile for the interaction and dilution of CTAB at pH 4. There were two breaks in the plots: an initial mild break with small f_{c_P} value, that corresponded to c_P of the system, and the second break corresponding to the c_S. Tensiometric cac was absent in the conductometric profiles. The results are presented in Tables 3 and 5. The c_P and c_S values increased mildly with pH for 5×10^{-5} kg dL^{-1} of pepsin but the increase was much more pronounced for 50×10^{-5} kg dL^{-1} of pepsin. The f_{c_S} declined with increasing [pepsin] whereas f_{c_P} increased. Both parameters showed an appreciable declining effect with pH for the higher [pepsin]. The structural and organizational differences between the two types of aggregates were considered to be the reason, deciphering of which is difficult at this stage. With variation in [pepsin] at pH 4, c_P increased gradually (opposite to the tensiometric finding), whereas c_S was very close to the tensiometric values (Table 4). The disagreement in c_P probably arose because the two methods probe two different physicochemical phenomena, tensiometry being sensitive to any change in interfacial composition and rheology, whereas conductometry measured any change in the number of charge carriers in the bulk solution phase.

TABLE 5: Conductometric and Microcalorimetric Observables in the Presence of 50×10^{-5} kg dL^{-1} of Pepsin at 303 K[a]

method		pH 3	pH 4	pH 6	pH 8
conductometry	c_P	0.62	0.64	0.74	0.78
	f_{cp}	0.41	0.39	0.36	0.30
	c_S	0.99	1.22	1.27	1.33
	f_{cs}	0.64	0.51	0.49	0.46
microcalorimetry	c_P		0.67	0.74	0.81
	ΔH_{cp}		−1.16	−1.52	−2.65
	c_S		1.18	1.26	1.36
	ΔH_{cs}		4.15	4.19	5.05
	cmc$_e$		1.67	1.75	1.81
	ΔH_{cmce}		−2.55	−2.95	−2.34

[a] c_P, c_S, and cmc$_e$ are given in mmol dL^{-1}, and ΔH values are given in kJ mol^{-1}. Standard deviations (SD) for cmc are ±3% and ±2% in conductometric and microcalorimetric methods. SD for ΔH is ±3%.

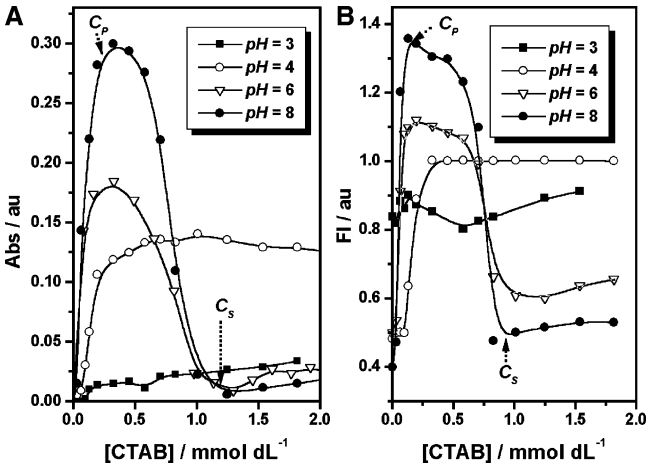

Figure 4. Variation in (A) absorbance and (B) fluorescence intensity at 303 K with dilution of CTAB in 5×10^{-5} kg dL^{-1} of pepsin at different pH.

C. Spectrophotometry: *Pepsin−CTAB interaction.* a. UV Spectrophotometry. Pepsin has a UV peak at 280 nm corresponding to the electronic transitions in the tryptophan and tyrosine residues, which remained unaltered in the presence of CTAB. The difference in absorbance at 280 nm between pepsin in CTAB and pure pepsin solution was plotted against [CTAB] in Figure 4A. At pH 3, absorbance of pepsin remained virtually unaffected on CTAB addition whereas at pH 4, the absorbance increased sharply up to c_P (0.2 mmol dL^{-1}, Table 3) and remained unaltered thereafter. The profiles at pH > 4 also increased sharply, reached a maximum at c_P, and decreased on the higher [CTAB] up to complete solubilization, c_S, and leveled off there. Similar turbidimetric findings were also reported by Hashidzume et al.[44] and Chen et al.[45] for interaction of surfactants with synthetic polymer. The above results suggested exposure of more tyrosine and tryptophan residues in pepsin at pH > 3 by the interaction with CTAB. The biopolymer became softer to expose the UV-active residues. At [CTAB] > c_P, the bound surfactant molecules in the form of clusters shielded (or screened) the residues from the radiation, causing the decline in absorbance.

b. Fluorimetry. The protein−surfactant interaction studies mostly utilized an external fluorophore, generally ANS.[7,8,46,47] We have studied the intrinsic tryptophan and tyrosine fluores-

TABLE 6: Determination of Free Energy of CTAB and 5×10^{-5} kg dL^{-1} of Pepsin−CTAB Mixtures at Different pH and That of the Mixtures with Different Pepsin Concentrations at 303 K[a]

	pure CTAB		5×10^{-5} kg dL^{-1} pepsin-CTAB mixtures			
pH	$-\Delta G^0_m$	$-\Delta G^0_{ad}$	$-\Delta G^0_{cac}$	$-\Delta G^0_{Cp}$	$-\Delta G^0_{Cs}$	$-\Delta G^0_{ad}$
3	55.1	71.1	33.3		49.6	60.4
4	48.5	64.3	32.3	60.2	47.1	63.0
6	47.1	65.8	35.6	61.7	47.0	71.9
8	46.0	66.9	36.4	63.1	46.5	83.1

[pepsin]/kg dL^{-1}	$-\Delta G^0_{cac}$	$-\Delta G^0_{Cp}$	$-\Delta G^0_{Cs}$	$-\Delta G^0_{ad}$
5×10^{-5}	32.3	36.6	48.0	63.0
10×10^{-5}	32.3	40.6	46.0	65.7
20×10^{-5}	35.6	46.5	44.2	62.8
25×10^{-5}	36.4	46.8	42.8	69.5
50×10^{-5}	37.4	45.4	40.8	56.0

[a] In all the ΔG^0 calculations we have considered the tensiometric values. cmc_e is observed only microcalorimetrically, its free energy calculation was omitted. $-\Delta G^0$ values are expressed in kJ mol^{-1}. Variation in [pepsin] was performed at pH 4.

cence[29,30] of pepsin following the line of Shweitzer et al.[19] The fluorescence intensity (FI) profiles at 360 nm against [CTAB] are presented in Figure 4B. The profiles were very similar to those observed in the UV−VIS spectroscopy discussed above. At pH 3, change in the spectral profile was not perceptible whereas at pH 4 there was an initial increase in FI near c_P (0.23 mmol dL^{-1}, Table 1), and it remained unaltered thereafter. At low pH, the protonated imidazole ring of the histidine moiety and the carboxyl groups quenched the fluorescence of tryptophan and tyrosine moieties.[48] At higher pH, a bell-shaped profile appeared. The increasing FI on increasing [CTAB] up to c_P at pH > 3 reflected the exposure of the tryptophan residues upon interaction with CTAB that attained a maximum at c_P. Further addition of CTAB shielded the residues from exposure to the radiation by the amphiphile aggregates and the FI declined and leveled off at c_S. In both the absorption and emission measurements, the formation of cac evidenced in tensiometry was absent.

3. Thermodynamics of Interaction. *A. General.* The free energy of micellization of pure CTAB was calculated by using

$$\Delta G^0_m = (1 + f)RT \ln X_{cmc} \quad (3)$$

where X_{cmc} and f are the cmc of pure CTAB in mole fraction scale at the respective pH and the extent of counterion condensation at the micellar surface, respectively, and the values are given in Table 6. The associated free energy changes at cac, c_P, and c_S were also calculated with similar equations, using f and X values of the respective states. In the calculation, we have used the cac, c_P, and c_S values from the tensiometric study and the degree of counterion condensation (f) as obtained from conductometry. As cac was not observed conductometrically, for calculation of ΔG^0_{cac}, the free energy equation was reduced to $\Delta G^0_{cac} = RT \ln X_{cac}$.

Gibbs surface excess for the pepsin−CTAB complex (Γ^{cs}_{max}) was calculated from eq 1, only replacing the limiting concentration from cmc to c_S, and the area of exclusion per pepsin−CTAB complex at the air/solution interface (A^{cs}_{min}) was calculated from eq 2. The Γ^{cs}_{max} and A^{cs}_{min} values at different conditions of the system are given in Tables 3 and 4. For 5×10^{-5} kg dL^{-1} of pepsin, Γ^{cs}_{max}decreased with increasing pH of the solution (Table 3), and Γ^{cs}_{max} values were also smaller than those in the absence of pepsin (Table 1). The A^{cs}_{min} (>A_{min}, in the absence of the biopolymer) increased with increasing pH. Variation in [pepsin] at pH 4 yielded no regular trend in Γ^{cs}_{max} and A^{cs}_{min}, as reported in Table 4.

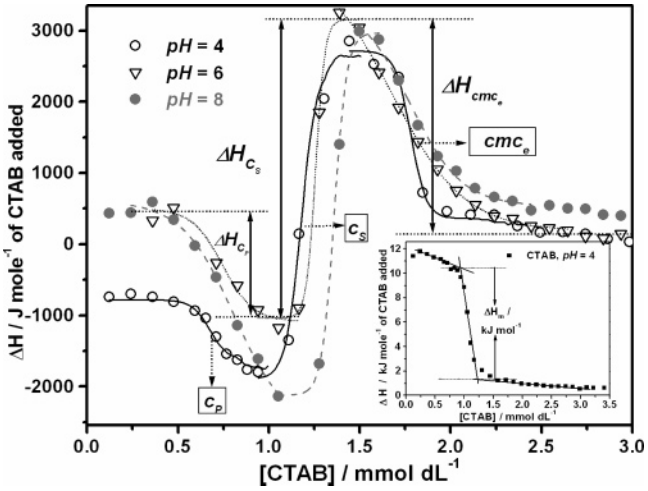

Figure 5. The microcalorimetric profiles of pepsin−CTAB interaction at 303 K for 50×10^{-5} kg dL^{-1} of pepsin at pH 4, 6, and 8. The inset shows the dilution experiment of pure CTAB at pH 4. Symbols represent the experimental points; lines are the fitted points obtained from the Sigmoidal Boltzmann Fitting procedure.

The free energy of adsorption at the air/solution interface was calculated from the equation

$$\Delta G^0_{ad} = \Delta G^0_{c^*} - \frac{\pi_{c^*}}{\Gamma_{c^*}} \quad (4)$$

where c* corresponds to a state of saturated monolayer formation at the air/solution interface, and π_{c^*} is the surface pressure at the saturated air/solution interface and was obtained by using $\pi_{c^*} = \gamma_0 - \gamma_s$, where γ_0 and γ_s are the surface tension values of initial solution (buffer for dilution isotherms and pepsin solution for interaction profiles) and that under complete monolayer formation and Γ_{c^*} is the Gibbs' surface excess at monolayer saturated air/solution interface. The free energy of adsorption values are reported in Table 6. It was found that the interfacial adsorption of the CTAB and that of CTAB−pepsin combine were more or less equally feasible. Also with increasing pH of the medium, the propensity of interfacial adsorption of the complex increased gradually, showing the predominant effect of electrostatic interaction. No such regularity was observed on varying [pepsin].

B. Microcalorimetry. a. Pure CTAB. Enthalpograms for dilution of CTAB in aqueous solution of different pH values have three distinctive courses of [CTAB] dependent variation in ΔH. At low [CTAB], there was a mildly decreasing part at higher ΔH; the higher ΔH value probably originated from the demicellization process and unfavored polar water−nonpolar hydrocarbon tail interaction of the surfactant. Finally, there was again a near-plateau in the enthalpograms, corresponding to the micellar dilution process. The intervening sharply decreasing stage corresponded to the micellization process. The small but finite width (in [CTAB]) of the micellization process signifies some change in morphology, micellar growth, etc. The threshold [CTAB] corresponding to the steeply decreasing ΔH was considered as the cmc of the surfactant. The vertical height at cmc between the demicellization stage and micellar dilution process was considered as the enthalpy of micellization, ΔH_m. Table 1 signifies only weak pH dependence of both cmc and ΔH_m.

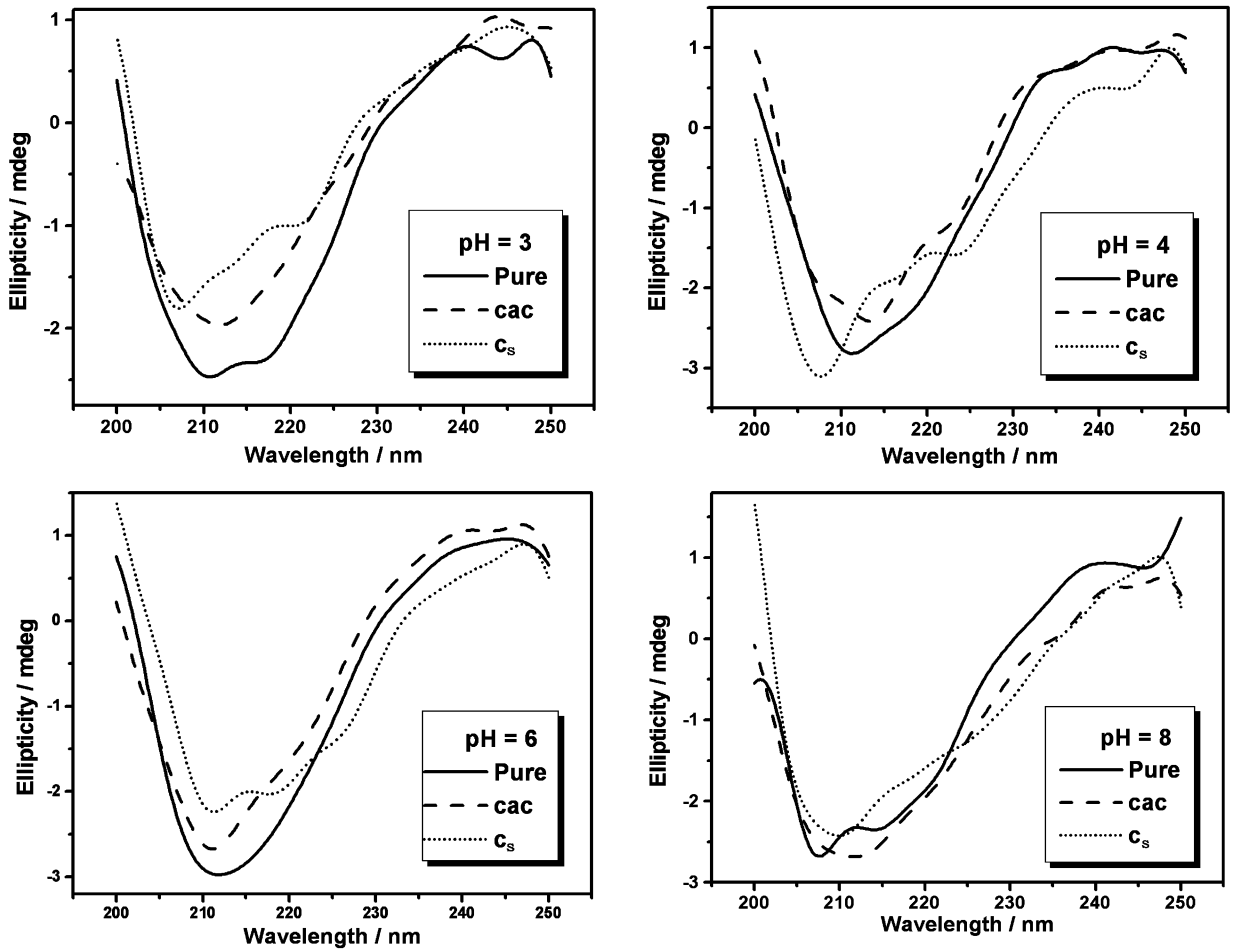

Figure 6. Far-UV CD spectra of pure pepsin and pepsin−CTAB mixtures (at 303 K) containing 5×10^{-5} kg dL^{-1} of pepsin at different pH values.

b. Pepsin−CTAB Interaction. The microcalorimetric experiments of interaction of CTAB with pepsin were performed at pH 4, 6, and 8 with 50×10^{-5} kg dL^{-1} of pepsin. The difference enthalpograms ($\Delta H = \Delta H^{pep}_{CTAB} - \Delta H^{H_2O}_{CTAB}$) are shown in Figure 5 (the inset representing the enthalpogram of CTAB dilution at pH 4).

The enthalpograms of pepsin−CTAB interaction consisted of three distinct courses: the first was an initial decline followed by a steep rise and another decline. The transition point in the initial sigmoidal decline corresponded to c_P, and the transition point in the subsequent increase in ΔH represented c_S. None of the other employed methods witnessed the formation of extended cmc, i.e., cmc_e. In fact the c_S values realized there were even to certain extents lower than the cmc of pure CTAB. The transition point in the final decline in enthalpy observed in the enthalpograms appeared like cmc_e as observed for interaction between surfactant and water-soluble polymers reported in the literature.[9,51−55] This feature did not match with the results by other methods. In previous sections, we have explained the absence of cmc_e in tensiometry because of interfacial saturation preferentially by the pepsin−CTAB complex; γ was brought to low values and further accommodation of amphiphile was not favored. The surfactant monomers aggregated in the bulk at [CTAB] > c_S without its manifestation on the interfacial tension. The result of an unchanged counterion binding probably failed also to show a break in the conductometric plot to manifest cmc_e. The property was revealed in calorimetry, which could register the enthalpy change for the aggregation process in the bulk phase and the third sigmoidal course stood for the extended micelle forming process. The gross enthalpy changes associated with the amphiphile−pepsin interaction were estimated with reference to the display at pH 6. The difference in enthalpies between the onset and saturation of the sigmoidal profile corresponded to the enthalpy change associated with the process. Enthalpy change for the different processes (ΔH_{c_P}, ΔH_{c_S}, andΔH_{cmc_e}) are shown in Figure 5.

All the enthalpy values are presented in Table 5. The process showed increased spontaneity with increased exothermicity on increasing pH. The enthalpy changes evidenced feeble dependence on pH. The binding-aggregation and micellization processes were exothermic, whereas the unfolding and consequent desorption of lower CTAB aggregates were endothermic and were in the expected enthalpic direction.

4. Structural Information of Pepsin−CTAB Interaction. The changes in the secondary and tertiary structures of pepsin at different stages of its interaction with CTAB under varied environmental conditions were studied by CD measurements. The spectra were taken in two different wavelength regions: (a) far-UV CD spectra (200−250 nm) and (b) near-UV CD spectra (250−320 nm). Figure 6 shows the far-UV CD spectra of 5×10^{-5} kg dL^{-1} of native pepsin and its mixture with CTAB at cac and c_S stages at different pH values. At pH 6, the far-UV CD spectra of the native pepsin evidenced a broad minima around 212 nm confirming a β-sheet-rich structure as reported by Gekko et al.[56,57] They reported that in 10 mmol dL^{-1} of phosphate buffer of pH 6.5, 0.01 kg dL^{-1} of pepsin consisted of 15.3% α-helix, 41.7% β-sheet, 20% turn, and the rest unordered. At pH 3, the spectrum of pure pepsin showed a hump near 220 nm along with a minimum at 212 nm indicating the high α-helical structure of the protein molecule. This hump

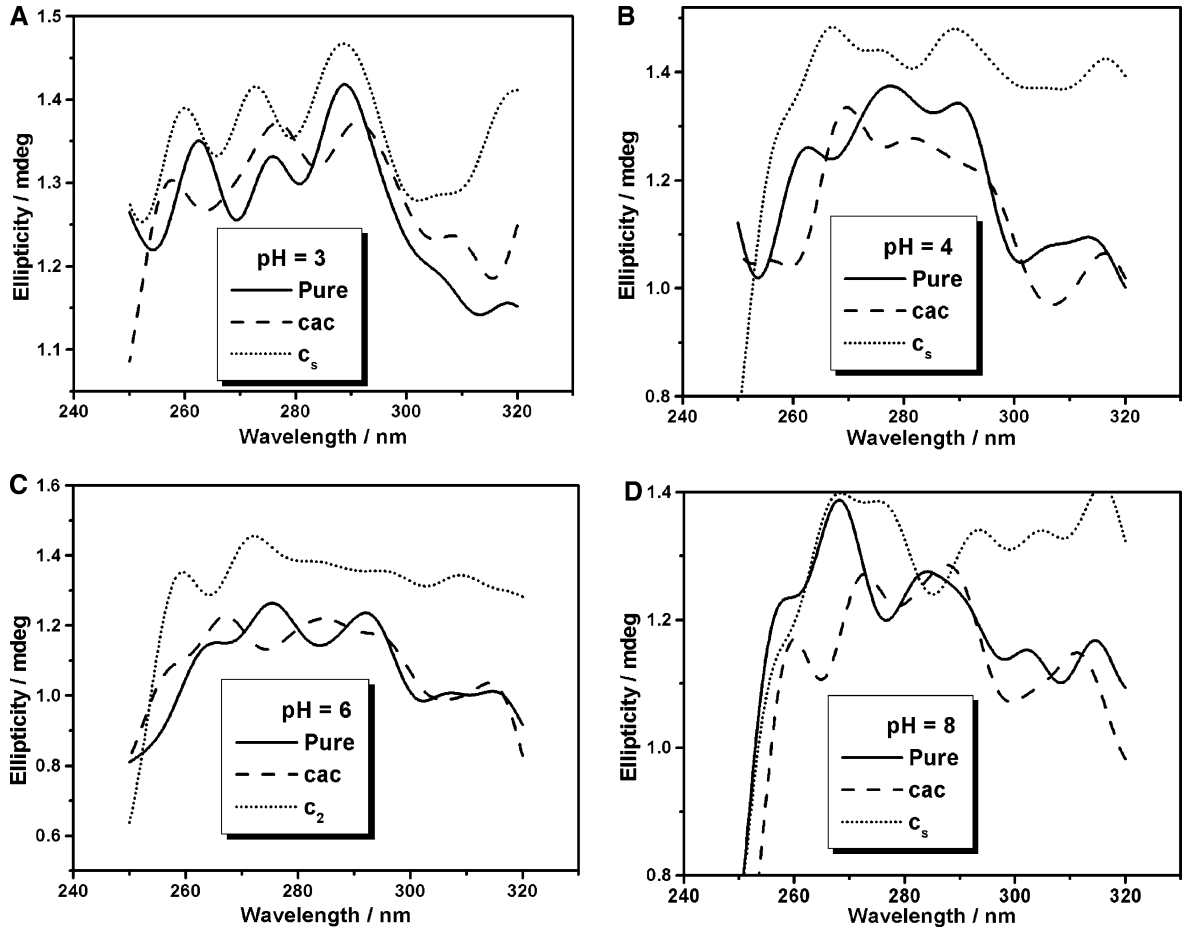

Figure 7. Near-UV CD spectra of pure pepsin and pepsin−CTAB mixtures (at 303 K) containing 5×10^{-5} kg dL^{-1} of pepsin at different pH values.

decreased and ultimately disappeared from the spectra of pure pepsin on increasing the pH from 3 to 6 due to partial transformation of the α-helix to the β-sheet. At pH 8, a large left-shifted minimum (from 212 to 207 nm) appeared indicating the partial unfolded structure and consequent denaturation of pepsin due to partial inactivity.

Addition of CTAB in pepsin solution at cac at different pH values did not produce perceptible spectral changes as depicted in Figure 6. Only a broadened band appeared near 211 nm on account of the β-sheet-rich structure. This observation was also in line with our inference that the CTAB monomer and small aggregates bind to the high-energy sites of the protein and populate the microdomain within the native protein structure. At the c_S stage, a sharp negative peak at 207 nm predominated with a small shoulder at 222 nm at pH 3 and 4. This can be assigned to the parallel excitations of the $\pi-\pi^*$ transitions of the peptide, and the $n-\pi^*$ transition of the carbonyl group of the peptide bond.[57] The sharp peak at 207 nm indicated α-helicity due to strong electrostatic repulsion, and decreased β-strand due to the partial unfolded structure of pepsin by the denaturating effect of CTAB. Similar behavior was observed for trypsin−SDS and papain−SDS systems.[27−30] It also confirmed cooperative binding and unwinding of the globular structure. The [CTAB] near c_S, therefore, induced a transition of the secondary structure from β-sheet to α-helix.

Near-UV CD spectra generated information on the aromatic amino acid residues and the disulfide bonds of protein. Figure 7 shows the near-UV CD spectra of native pepsin (5×10^{-5} kg dL^{-1}) and that along with CTAB at cac and c_S stages at different pH values (3, 4, 6, and 8). The intensity of the spectra of disulfide bonds between cystein residues of protein may be calculated from the following three factors: (1) the dihedral angle of the disulfide bonds, (2) the C−S−S bond angle, and (3) the interaction with the protein matrix.[58] From the reported amino acid sequence,[59] pepsin contains three S−S linkages between (45−50), (206−210), and (250−283) cystein residues, which is reflected in the near-UV positive CD spectra of native pepsin in all pH values in the wavelength range of 257−292 nm. With increasing pH of the solution, the spectra of native pepsin gradually changed due to breaking of the disulfide bridges. At pH 3, the two distinct minima were obtained near 267 and 280 nm for the mixtures in both cac and c_S conditions as in the case of native pepsin. At pH 4, the first minimum of the mixture was red-shifted and the second became very faint at cac with increased intensity at c_S. At pH 6, an almost similar pattern was obtained at cac whereas at c_S the first minimum was pronounced and the second becomes almost flat. At pH 8, the minima were, however, much more pronounced at cac compared to that of the native pepsin, ensuring an increase in compactness of the polymer−surfactant aggregates. The enhanced intensity of the minima at c_S denoted a change of tertiary structure, especially the loss in asymmetry around the disulfide bridges and the changes in the environment of the tryptophan residue.[60] Pepsin was, therefore, less compact at c_S compared to its native state.

Overall Remarks

Pure native pepsin is solubilized in water through hydration at its peripheral ionic sites as shown in Scheme 1A. The general feature of pepsin−CTAB interaction can be divided into four

stages (Scheme 1B−E). At the low [CTAB] regime, surfactant monomers preferentially adsorb on to the oppositely charged peripheral pepsin sites with a concomitant increase in hydrophobicity. This interaction increases the stability of the native structure of the biopolymer, resulting in an increased compactness in globular structure. Monomeric CTA^+ adsorption to these ionic sites results in depletion of water of solvation and increased hydrophobicity of the overall complex as observed from the viscosity and CD study. The increased hydrophobicity makes the biopolymer−CTAB complex prone to interfacial adsorption, leading the process to be sensitive to γ (as shown in Scheme 1B). This interaction cannot affect the state of counterion binding of the aggregate compared to the monomeric surfactant in solution, and so could not be experienced conductometrically. Microcalorimetry failed to detect cac indicating the process was not perceptibly enthalpy producing.

Addition of further CTAB led to coacervation and turbidity of the solution. This coacervation depleted the biopolymer−surfactant complex from the interface, leading to a nominal increase in γ (Scheme 1C). The process reaches its limit at the maximum in the tensiometric isotherm (c_P). c_P also pointed to the threshold [CTAB] to induce unfolding of native pepsin to expose more binding sites for the surfactant, offering a polar environment to the fluorophoric amino acid residues of the biopolymer, which makes the process spectroscopically explorable. The phase-out phenomenon also affects the ion transport behavior in the solution, pointing its detection conductometrically. The process was also enthalpically sensitive as observed from the microcalorimetric study with 50×10^{-5} kg dL^{-1} of pepsin.

The unfolding of the biopolymer at c_P induced further surfactant adsorption on to the pepsin sites, both in monomeric and aggregated forms (Scheme 1, D), which favorably populated at the air/solution interface with a concomitant lowering in γ. The saturation in γ means that no more pepsin−CTAB complex is available for interfacial adsorption, pertaining to the saturation binding of CTAB to the biopolymer, c_S. Formation of lower surfactant aggregates below the cmc of pure CTAB is driven by an increase in local [CTAB] in the vicinity of the biopolymer, which may also reach the cmc of the free surfactant in the absence of the biopolymer. The break in the conductometric profile at c_S was consistent with the formation of lower surfactant aggregates at this stage of interaction (Scheme 1, D). We suggest a threadlike structure of the unfolded biopolymer penetrating the lower surfactant aggregates pertaining to a necklace structure.[8] The above rationalized unfolded and less compact pepsin structure was also supported by the viscometric and CD spectra. The decrease in spectral intensity is expected to result from the shielding of the fluorophoric moiety by the surfactant aggregates from the influence of excitation. The process was endothermic as revealed by microcalorimetry and is found to be mostly enthalpy oriented.

Addition of CTAB beyond c_S resulted in competitive interfacial adsorption of the polymer−surfactant aggregate and free monomeric CTAB. Because of higher interfacial affinity of the pepsin−CTAB complex than the free CTAB, the latter could not deplete the pepsin−CTAB complex from the air/solution interface as evidenced from lower γ_{c_S} than γ_{cmc}. The accumulated free CTAB monomers in the bulk solution consequently associated to form free micelle in bulk solution (Scheme 1, E), without affecting the interface. Because of similar f of the CTAB aggregates in pure and in pepsin-bound states, conductometry was insensitive to detect the free micelle formation, i.e., extended critical micellar concentration (cmc_e). The process did not involve the pepsin and hence could not be probed by spectrophotometry and viscometry. However, microcalorimetry monitored the process successfully because it was a direct energy involving method. Variation in pH of the medium produced the expected results caused by increased charge density of the biopolymer. An increase in negative charge density of the biopolymer at increased pH intensified the extent of interaction.

Acknowledgment. T.C. and I.C. thank CSIR, Government of India, for financial assistance and S.P.M. thanks INSA for an Honorary Scientist position.

References and Notes

(1) Ananthapadmanabhan, K. P. In *Interactions of Surfactants with Polymers and Proteins*; Goddard, E. D., Ananthapadmanabhan, K. P., Eds.; CRC Press, Inc.: London, UK, 1993; Chapter 8.
(2) Reynolds, J. A.; Tanford, C. *J. Biol. Chem.* **1970**, *245*, 5161−5165.
(3) Tanford, C. *J. Mol. Biol.* **1972**, *67*, 59−74.
(4) Shirahama, K.; Tsujii, K.; Takagi, T. *J. Biochem.* (*Tokyo*) **1974**, *75*, 309−314.
(5) Jones, M. N.; Manley, P. *J. Chem. Soc., Faraday Trans. 1* **1979**, *75*, 1736−1744.
(6) Jones, M. N. *Biochem. J.* **1975**, *151*, 109−114.
(7) Griffiths, P. C.; Roe, J. A.; Bales, B. L.; Pitt, A. R.; Howe, A. M. *Langmuir* **2000**, *16*, 8248−8254.
(8) Turro, N. J.; Lie, X.-G.; Ananthapadmanabhan, K. P.; Aronson, M. *Langmuir* **1995**, *11*, 2525−2533.
(9) Kelley, D.; McClements, D. J. *Food Hydrocolloids* **2003**, *17*, 73−85.
(10) Moriyama, Y.; Takeda, K. *Langmuir* **2005**, *21*, 5524−5528.
(11) Vasilecu, M.; Angelescu, D.; Almgren, M.; Valstar, A. *Langmuir* **1999**, *15*, 2635−2643.
(12) Honda, C.; Kamizono, H.; Matsumoto, K.; Endo, K. *J. Colloid Interface Sci.* **2004**, *278*, 310−317.
(13) Deep, S.; Ahluwalia, J. C. *Phys. Chem. Chem. Phys.* **2001**, *3*, 4583−4591.
(14) Palacios, A. C.; Antonelli, M. L.; La Mesa, C. *Thermochim. Acta* **2004**, *418*, 69−77.
(15) Gani, S. A.; Mukherjee, D. C.; Chattoraj, D. K. *Langmuir* **1999**, *15*, 7139.
(16) Biswas, S. C.; Chattoraj, D. K. *Langmuir* **1997**, *13*, 4505.
(17) Biswas, S. C.; Chattoraj, D. K. *Langmuir* **1997**, *13*, 4512.
(18) Maulik, S.; Dutta, P.; Chattoraj, D. K.; Moulik, S. P. *Colloid Surf. B* **1998**, *11*, 1−8.
(19) Shweitzer, B.; Zanette, D.; Itri, R. *J. Colloid Interface Sci.* **2004**, *277*, 285−291.
(20) Gelamo, E. L.; Itri, R.; Alonso, A.; da Silva, J. V.; Tabak, M. *J. Colloid Interface Sci.* **2004**, *277*, 471−482.
(21) Honda, C.; Kamizono, H.; Matsumoto, K.; Endo, K. *J. Colloid Interface Sci.* **2004**, *278*, 310−317.
(22) Green, R. J.; Su, T. J.; Joy, H.; Lu, J. R. *Langmuir* **2000**, *16*, 5797−5805.
(23) Lad, M. D.; Ledger, V. M.; Briggs, B.; Green, R. J.; Frazier, R. A. *Langmuir* **2003**, *19*, 5098−5103.
(24) Fraizier, R. A.; Papadopoulou, A.; Mueller-Harvey, I.; Kissoon, D.; Green, R. J. *J. Agric. Food Chem.* **2003**, *51*, 5189−5195.
(25) Chatterjee, A.; Moulik, S. P.; Majhi, P. R.; Sanyal, S. K. *Biophys. Chem.* **2002**, *98*, 313−327.
(26) Stenstam, A.; Khan, A.; Wennerstrom, H. *Langmuir* **2001**, *17*, 7513−7520.
(27) Ghosh, S.; Banerjee, A. *Biomacromolecules* **2002**, *3*, 9−16.
(28) Ghosh, S. *J. Surf. Sci. Technol.* **2003**, *19*, 167−181.
(29) Ghosh, S. *Colloid Surf. A* **2005**, *264*, 6−16.
(30) Ghosh, S. *Colloid Surf. B* **2005**, *41*, 209−216.
(31) Ghosh, S. Private communication.
(32) Brewer, M.; Scott, T. *Concise Encyclopidia of Biochemistry*, Translation of Brockhans, ABC Biochemie; Jakubke, H. D., Jeschkeit, H., Eds.; Walter de Gruyter Publishers: Berlin, Germany, 1983; Vol. 30, p 331.
(33) Tang. J.; Sepuleva, P.; Marciniszyn, J.; Chen, K. C. S.; Huang, W.-Y.; Tao, N.; Liu. D.; Lanier, J. P. *Proc. Natl. Acad. Sci. U.S.A.* **1973**, *70*, 3437−3439.
(34) Moulik, S. P.; Ghosh, S. *J. Mol. Liq.* **1997**, *72*, 145−161.
(35) Ghosh, S.; Moulik, S. P. *J. Colloid Interface Sci.* **1998**, *208*, 357−366.
(36) Ghosh, S. *J. Colloid Interface Sci.* **2001**, *244*, 128−138.
(37) Chakraborty, T.; Ghosh, S.; Moulik, S. P. *J. Phys. Chem. B* **2005**, *109*, 14813−14823.

(38) Peyere, V.; Lair, V.; Andre, V.; la Marie, G.; Kragh-Hansen, U.; le Maire, M.; Moller, V. *Langmuir* **2005**, *21*, 8865−8875.
(39) Jean, B.; Lee, L. T.; Cabane, B. *Langmuir* **1999**, *15*, 7585−7590.
(40) Asnacios, A.; Langevin, D.; Argillier, J. F. *Macromolecules* **1996**, *29*, 7412−7417.
(41) Deo, P.; Somasundaran, P. *Langmuir* **2005**, *21*, 3950−3956.
(42) Chakraborty, T.; Cakraborty, I.; Ghosh, S. *Langmuir* **2006**, *22*, 9905−9913.
(43) Cabane, B.; Duplessix, R. *J. Phys.* (*Paris*) **1982**, *43*, 1529−1533.
(44) Hashidzume, A.; Ohara, T.; Morishima, Y. *Langmuir* **2002**, *18*, 9211−9218.
(45) Chen, L.; Yu, S.; Kagami, Y.; Gong, J.; Osada, Y. *Macromolecules* **1998**, *31*, 787−794.
(46) Matulis, D.; Baumann, C. G.; Bloomfield, V. A.; Lovrien, R. E. *Biopolymers* **1999**, *49*, 451−458.
(47) Lakowicz, J. R. *Principles of Fluorescence Spectroscopy*, 2nd ed.; Plenum: New York, 1996; Chapter 16.
(48) Dockal, M.; Carter, D. C.; Ruker, F. *J. Biol. Chem.* **2000**, *275*, 3042−3050.
(49) Purcell, I. P.; Thomas, R. K.; Penfold, J.; Howe, A. M. *Colloids Surf. A* **1995**, *94*, 125−130.
(50) Buckingham, J. H.; Lucassen, J.; Hollway, F. *J. Colloid Interface Sci.* **1978**, *67*, 423−431.
(51) Thongngam, M.; McClements, D. J. *Langmuir* **2005**, *21*, 79−86.
(52) Romani, A. P.; Gehlen, M. H.; Itri, R. *Langmuir* **2005**, *21*, 127−133.
(53) Dai, S.; Tam, K. C. *Langmuir* **2004**, *20*, 2177−2183.
(54) Loh, W.; Teixeira, L. A. C.; Lee, L.-T. *J. Phys. Chem. B* **2004**, *108*, 3196−6201.
(55) Bai, G.; Nichifor, M.; Lopes, A.; Bastos, M. *J. Phys. Chem. B* **2005**, *109*, 518−525.
(56) Gekko, K.; Yonehara, R.; Sakurada, Y.; Matsuo, K. *J. Electron Spectrosc.* **2005**, *144*−*147*, 295−297.
(57) Matsuo, K.; Yonehara, R.; Gekko, K. *J. Biochem.* **2004**, *135*, 405−411.
(58) Strickland, E. H. *CRC Crit. Rev. Biochem.* **1974**, *2*, 113−175.
(59) Sepulveda, P.; Marciniszyn, J.; Liu, D.; Tang, J. *J. Biol. Chem.* **1975**, *250*, 5082−5088.
(60) Sun, C.; Yang, J.; Wu, X.; Huang, X.; Wang, F.; Liu, S. *Biophys. J.* **2005**, *88*, 3518−3524.